ACS APPLIED ELECTRONIC MATERIALS

pubs.acs.org/acsaelm Letter

Photoconductive Thin Films Composed of Environmentally Benign $AgBiS_2$ Nanocrystal Inks Obtained through a Rapid Phase Transfer Process

Mathew L. Kelley, Fiaz Ahmed, Sakiru L. Abiodun, Mohammad Usman, Mohi Uddin Jewel, Kamal Hussain, Hans-Conrad zur Loye, M. V. S. Chandrashekhar, and Andrew B. Greytak*

Cite This: *ACS Appl. Electron. Mater.* 2021, 3, 1550−1555 Read Online

ACCESS | Metrics & More | Article Recommendations | Supporting Information

ABSTRACT: We demonstrate a fast solution phase ligand exchange process to generate $AgBiS_2$ nanocrystal inks using a cinnamic acid derivative as an additive to accelerate the phase transfer to polar solvents. Photoconductivity in thin films assembled from the $AgBiS_2$ nanocrystal inks is achieved by using a single deposition step, avoiding multiple layer iterations. The inks remain colloidally stable after several days, and photoconductor devices showcase fast response times <4 ms, high on/off ratios ~20, and film conductivities of ~3 × 10^{-8} S/cm, highlighting the promise in completely solution processed thin film electronics and optoelectronics using eco-friendly materials.

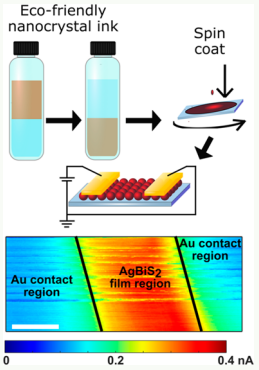

KEYWORDS: *ternary semiconductor, quantum dot, photoconductive, thin film, phase transfer*

Colloidal semiconductor quantum dots (QDs) have garnered great interest for next-generation solar cells and photodetectors in recent decades due to their size tunable optical properties, compatibility with solution processing, and applicability to flexible substrates. These favorable characteristics engender the realization of low cost and scalable devices with architectures inaccessible to conventional crystalline semiconductors. Although lead and cadmium chalcogenide QDs are the most widely studied and well-understood types of QDs,[1] the advancement of environmentally friendly alternatives is crucial to minimize toxicity hazards and achieve compliance with regulatory directives.

The ternary semiconductor $AgBiS_2$ is an appealing eco-friendly candidate for optoelectronics.[2,3] $AgBiS_2$ is a type I−III−VI semiconductor with a favorable characteristics for solar photovoltaics including a narrow bulk bandgap of ~0.8 eV,[4] a large absorption coefficient (~10^5 cm^{-1}),[5] and giant static dielectric constant (~10^5).[6] $AgBiS_2$-based devices have demonstrated promising performance in recent studies. Notably, heterojunction solar photovoltaics with an $AgBiS_2$ active layer achieved a power conversion efficiency of 6.3%,[5] and hybrid $AgBiS_2$ QD/graphene phototransistors[7] with responsivities of ~10^5 A/W were reported. However, nearly all $AgBiS_2$ device reports to date have undertaken a solid-state ligand exchange (SSLE) step during film assembly to achieve conductive thin films. Although the native long-chain ligands terminating the surface of QDs maintain colloidal stability in nonpolar solvents after synthesis, the ligands function as electrically insulating media in assembled films and impede carrier collection, which limits the device performance.[8] The ubiquitous strategy to overcome this is to replace the bulky ligands with shorter ligands, which reduces the separation distance between neighboring QDs and enhances electronic coupling, ultimately improving charge transport in the film. Although SSLE processes by spin coating are effective strategies in laboratory contexts, on larger scales throughput is limited by successive multilayer deposition iterations, which ensures that film continuity is maintained and not impinged by the stochastic formation of cracks and voids that emerge during SSLE steps. In addition, SSLE methods are completely incompatible with large area fabrication, underscoring its confinement to research settings.[9] To achieve widespread deployment of QD-based devices, it is critical to develop solution-phase exchange approaches compatible with high-output single-step deposition processes such as inkjet printing or spray coating.

Received: December 18, 2020
Accepted: April 13, 2021
Published: April 16, 2021

https://doi.org/10.1021/acsaelm.0c01107
ACS Appl. Electron. Mater. 2021, 3, 1550−1555

Many approaches for solution-phase replacement of native, long chain, electrically insulating ligands at QD surfaces have been developed. In early work by the Kagan and Murray groups,[10] a flocculation-based method was utilized to exchange trioctylphosphine oxide or oleic acid ligands at semiconductor and metallic nanocrystal surfaces with thiocyanate ligands, with suspension in polar solvents such as dimethyl sulfoxide. Lateral thin film photodetectors of thiocyanate-capped CdSe QDs using this method achieved a photoconductivity as high as 10^{-5} Ω^{-1} cm^{-1}.[10] A flocculation-based approach was also applied to oleate-capped PbSe QDs,[11] wherein treatment with ammonium halides yielded electrostatically stabilized dispersions in several polar solvents including *N*-methylformamide, propylene carbonate, *N*,*N*-dimethylformamide, and formamide.[11] The Talapin group utilized a phase transfer method to exchange native ligands at nanocrystal surfaces with short metal chalcogenide, halide, pseudohalide, and halometallate ligands.[12,13] The method was successful in generating stable dispersions of metal chalcogenide QDs and was extended to III−V QDs and CdSe nanorods.[12,13] In PbS QDs, direct mixing of ligand solutions with QDs capped with native ligands has proven successful with cinnamic acid derivatives[14] as well as benzoic acid and 4-methylbenzoic acid.[15] Solution phase exchange of oleate with functionalized arenethiolate ligands was also reported for PbS QDs,[16] where a triethylammonium additive was employed to drive equilibrium toward generation of free thiolates and promote the displacement of bound oleate ligands. A two-step surface modification strategy was applied to InAs[17] QDs to tune the absolute band edge energy levels in assembled films. Finally, a two-step[18] cascade ligand treatment sequence was used to generate PbS QD inks suitable for bulk heterojunction solar photovoltaics in a recent report. By and large, phase transfer[19] ligand exchange methods have dominated the QD solar photovoltaic domain, with lead halides[20] most frequently used to stabilize n-type PbS QD inks and passivate the QD surfaces.

Although PbS QDs are the most widely studied semiconductor for QD optoelectronics, innovations in solution-phase exchange techniques have been developed for ternary QDs as well. Choi et al. applied a phase transfer process to $AgSbS_2$ QDs[21] to generate stable dispersions in *N*-methylformamide. Reinhold et al. applied a new strategy to $CuInS_2$ nanoparticles by directly combining the dried particles with pure 4-methylbenzenethiol with subsequent dispersion in chlorobenzene.[22] Very recently, the generation of $AgBiS_2$ inks was demonstrated by using halometallate-based ligands in a phase transfer process, and the authors achieved power-conversion efficiencies as high as 4.08% in vertical photovoltaic devices.[23] Inspired by recent advancements in producing ternary QD inks for optoelectronics, we sought a strategy to accelerate the generation of stable $AgBiS_2$ inks and investigate the fundamental properties and response of films in photodetection contexts. It was recently found that the addition of hydroiodic acid during PbS QD phase transfer ligand exchanges with lead halides strongly accelerated the transfer of QDs to the polar solvent phase.[24] The hydroiodic acid served a dual functionality where it simultaneously behaved as a strong proton source to liberate bound olefin species and provided additional iodide ions to passivate the QD surface. However, despite the promising mechanism of the acid-assisted phase transfer exchange, strong acids such as hydroiodic acid pose nontrivial safety risks, and we were motivated to identify alternatives to apply to a ternary, environmentally benign QD system. Here, we find that the inclusion of a cinnamic acid derivative to ammonium halide ligand solutions dramatically accelerates the phase transfer ligand exchange process and yields stable colloidal inks. We assemble lateral thin film devices from the inks, study the fundamental conductivity and photoconductive behavior of the films by scanning photocurrent microscopy (SPCM), and find that fast (milliseconds) photoresponse times are achieved in simple photodetector devices.

The preparation of our $AgBiS_2$ ink is outlined in Scheme 1. Oleate-capped $AgBiS_2$ QDs were synthesized following a reported colloidal method with slight modifications.[5] The crude QD product was purified by a single precipitation−centrifugation−redispersion cycle under air-free conditions using low-toxicity methyl acetate[25] as the antisolvent with a final dispersion in octane. Figure 1a shows the powder X-ray diffraction (XRD) pattern of purified QDs overlaid with the calculated pattern for cubic $AgBiS_2$,[7,26,27] confirming the structure and phase purity of the material. To generate ligand exchanged $AgBiS_2$ inks, a phase transfer process using NH_4I salts in *N*,*N*-dimethylformamide (DMF) was adapted from the literature.[28] In brief, ammonium iodide was dissolved in DMF. Purified QDs in octane were added to the DMF solution, and the biphasic mixture was shaken vigorously to facilitate complete transfer to the DMF phase. Notably, we found that the inclusion of *trans*-4-(trifluoromethyl)cinnamic acid (4-CF_3) to the ammonium iodide ligand solution rapidly accelerated the phase transfer process from over an hour to less than 5 s, similar to acid-assisted phase transfer processes with PbS QDs.[24] Transmission electron microscopy (TEM) confirmed the phase transfer to DMF while retaining nanoparticle form (Figure 1b), indicating that the phase transfer process has not caused significant agglomeration. We propose that the 4-CF_3 additive functions similarly to hydroiodic acid in phase transfer processes, where the acidic 4-CF_3 proton liberates oleate ligands from the $AgBiS_2$ QDs and copassivates the surfaces with iodide ligands.

The phase transferred $AgBiS_2$ QDs were also characterized by absorbance spectroscopy (Figure 2). The pre- and post-phase transfer absorbance profiles of dispersed samples were free of obvious changes, signifying that the phase transfer did not diminish the optical properties of the $AgBiS_2$QDs. A Tauc plot (Figure 2b and Figure S1) generated from the phase transferred $AgBiS_2$ QD film confirmed the indirect bandgap of ∼1.08 eV.[4] We also observed that the phase transferred $AgBiS_2$ was relatively stable, as noted by the absorption profile of

Scheme 1. Formation of $AgBiS_2$ Ink through Synthesis, Purification, and Phase Transfer Ligand Exchange Steps

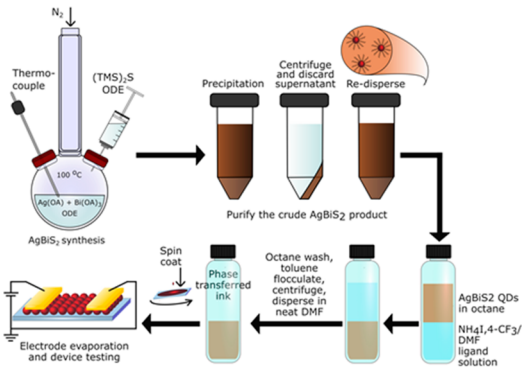

https://doi.org/10.1021/acsaelm.0c01107
ACS Appl. Electron. Mater. 2021, 3, 1550−1555

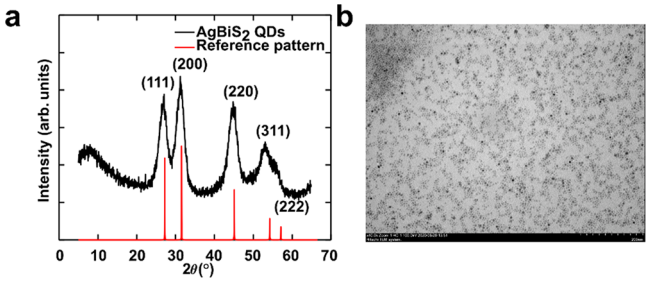

Figure 1. (a) XRD patterns of phase transferred $AgBiS_2$ QDs and calculated cubic $AgBiS_2$ reference (ICSD #AgBiS2-1959).[25] (b) TEM image of phase- transferred $AgBiS_2$ QDs.

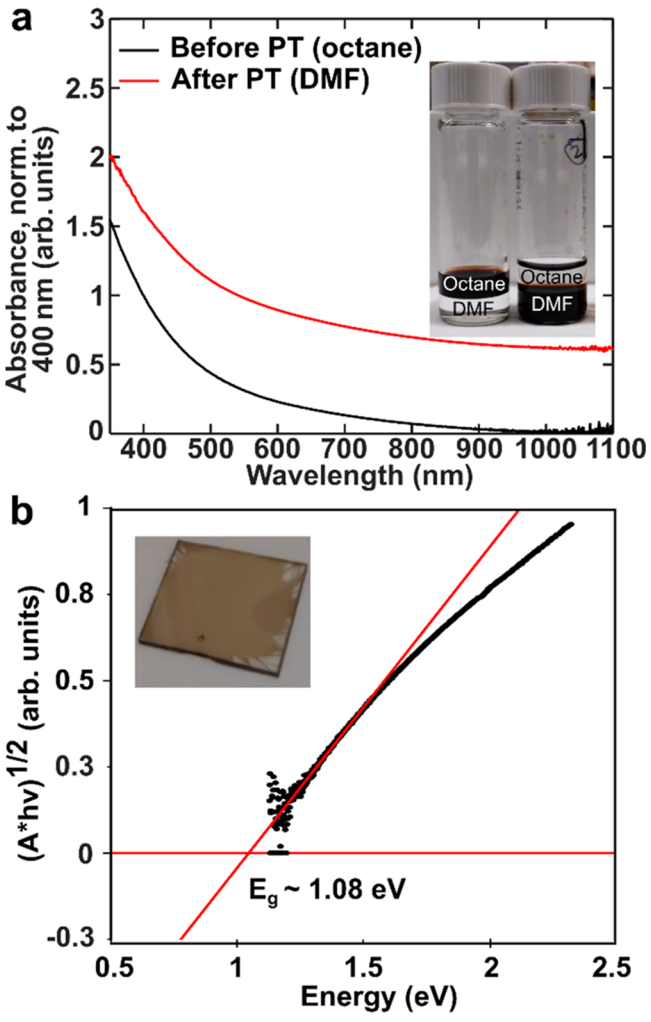

Figure 2. (a) Absorbance spectra of $AgBiS_2$ QDs prephase transfer (black) and postphase transfer. Spectra are normalized to 400 nm and vertically offset for clarity. Inset: images of prephase transfer and postphase transfer QDs showing transfer to the ligand−DMF phase. (b) Tauc plot of a $AgBiS_2$ QD film generated from the ink. The bandgap (E_g) is obtained from linear extrapolation to the baseline. Inset: image of a phase transferred $AgBiS_2$ film deposited on a transparent glass substrate.

dispersed QDs after several days storage time shown in Figure S2, although aggregation occurred over a longer period.

To obtain chemical information about the $AgBiS_2$ ink, we employed scanning electron microscopy (SEM) and energy dispersive X-ray spectroscopy (EDX) elemental mapping. Figure 3a shows a scanning electron micrograph of a spin-coated phase transfer film deposited onto a cleaned glass slide. We purposely chose this region of the sample to differentiate the film from the substrate, which was partially exposed by a scratch. The elemental maps for localized Ag, Bi, and S signals are consistent with the SEM micrograph. Importantly, elemental maps for I and F confirmed the presence of iodine and fluorine as anticipated from the halide and 4-CF_3 ligands used for the phase transfer exchange. We also observed that thicker (thinner) regions of the film were clearly distinguished by relatively higher (lower) localized signals in the Ag, Bi, S, I, and F elemental maps. Finally, the higher intensity signal in the Si elemental map showed a clear contrast between regions holding the continuous film and the exposed underlying substrate, confirming that other signals originated from the deposition of the phase transferred $AgBiS_2$ QD film.

Having ascertained the optical and chemical characteristics of the phase transferred ink, simple two terminal devices were used to examine the optoelectronic responses of films cast from the $AgBiS_2$ ink. Films were deposited on clean glass substrates under ambient conditions in a single spin-coating deposition step (see the Supporting Information for details). Metal (Au) top contacts were evaporated directly onto the film through a shadow mask to define device regions. Current−voltage (I−V) measurements at DC were taken to investigate the fundamental conductivity of the films and the DC photoresponse. From the dark I−V curves of these lateral devices (Figure 4a), the conductivity (σ) was obtained by the relation $\sigma = \rho^{-1}$, with $\rho = R(A/L)$, R is the resistance in ohms, L is the channel length between contacts, and A is the cross-sectional film area defined by the film thickness (~94 nm) and channel width. The films showed $\sigma \sim 3 \times 10^{-8}$ S/cm, comparable to early PbS QD[29] films generated in SSLE processes with dithiols and recently published work on dip-coated, ternary $NaBiS_2$ QD thin films.[30] A modest photocurrent of ~1 nA at 10 V bias was observed under wide-area steady-state illumination at 444 nm (power density ~2.7 mW/cm^2). High on/off ratios ~20 for the devices were observed from the photocurrent to dark current ratio ($I_{ph}/I_{dark} \sim 1$ nA/0.05 nA). Notably, the on/off ratios were relatively higher than lateral $AgBiS_2$ thin films formed from molecular precursors at higher temperatures and in multilayer deposition steps.[26,31]

We employed SPCM to examine the localized photocurrent generation in our lateral $AgBiS_2$ devices using a setup described previously.[32] SPCM is a powerful imaging technique that has been used to reveal information about carrier collection and local device responses in PbS QD devices.[33] Figure 4b shows a SPCM map of a $AgBiS_2$ device under 444 nm photoexcitation. We observed that the majority of photocurrent is generated within the channel region, indicative of photoconductive behavior.[33] In the context of photodetection, consistent and repeatable responses to input stimuli are necessary to achieve. To examine the reversibility and stability of our device photoresponses, we conducted photocurrent transient measurements on the devices. As displayed in Figure 4c, the reproducibility in the device response was evident in the photocurrent transients taken under 444 nm wide-area illumination (power density ~6.7 mW/cm^2), and consistent on/off ratios ~20 were maintained for several cycles. Another metric for photodetection contexts is the device response time. We found that our $AgBiS_2$ QD photoconductors were fast, with ~90% of the photocurrent decays occurring within <~4 ms as shown in Figure 4d. The fast response speed, high on/off

https://doi.org/10.1021/acsaelm.0c01107
ACS Appl. Electron. Mater. 2021, 3, 1550−1555

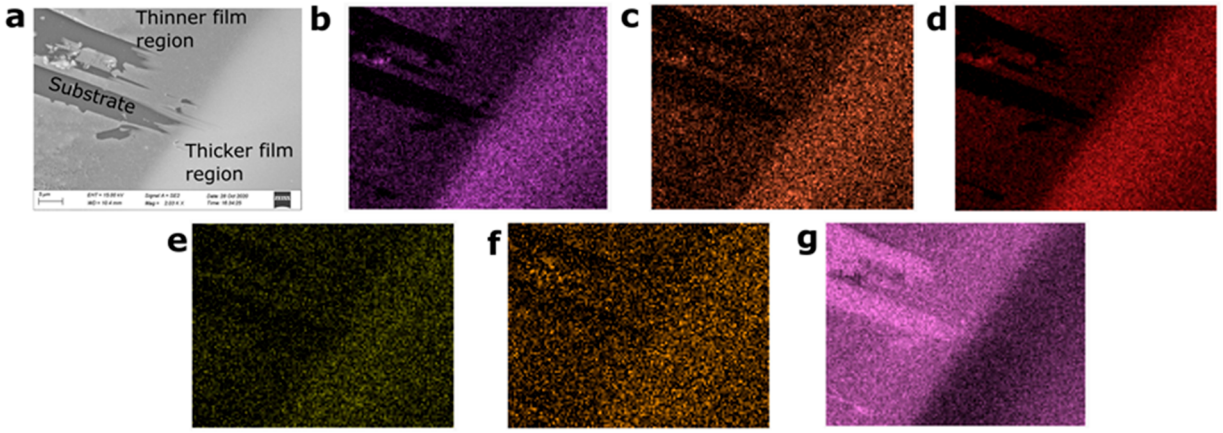

Figure 3. Energy-dispersive X-ray (EDX) spectroscopy of a phase transferred $AgBiS_2$ QD thin film. (a) shows the scanning electron microscopy (SEM) image taken at the edge of the substrate region with a scratch for contrast. SEM-EDX elemental mapping images for (b) S, (c) Ag, (d) Bi, (e) I, (f) F, and (g) Si for the film view shown in (a). The elevated Si intensity in (g) at the location where the film has been scratched away arises from the underlying glass substrate.

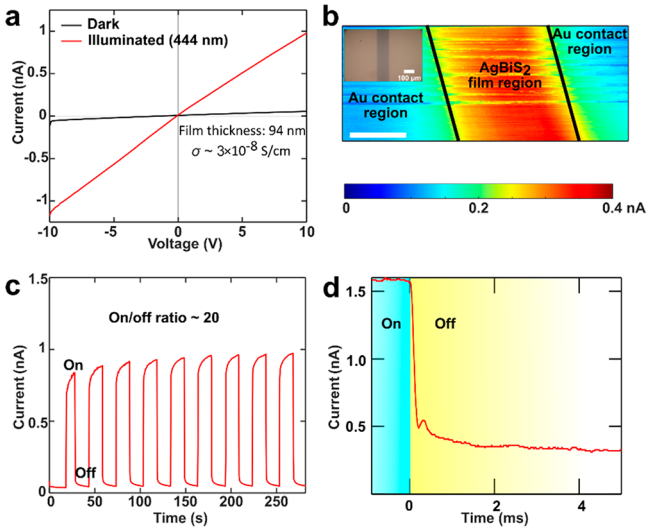

Figure 4. (a) Dark (black) and 444 nm illuminated (red) *I*−*V* curves for a thin film device obtained from the NH_4I/4-CF_3−$AgBiS_2$ ink. (b) SPCM of $AgBiS_2$ device (444 nm, 71 Hz). Black lines indicate electrode edges. Scale bar is 50 μm. Inset: optical microscope image of a lateral $AgBiS_2$ device showing Au contacts and the bridging $AgBiS_2$ film region; scale bar 100 μm. (c) Photocurrent transients taken on a thin film device at 10 V bias with 444 nm photoexcitation. (d) Transient at millisecond time scale.

ratio, and reversible photocurrent response highlight the promise of these environmentally benign $AgBiS_2$ inks for use in solution processed optoelectronics.

In conclusion, we have demonstrated a method for the rapid generation of eco-friendly $AgBiS_2$ QD inks. A fast phase transfer process was used to generate the QD ink, and suspensions of the phase transferred QDs were colloidally stable for several days. We have shown that photoconductivity in thin films formed from the ligand exchanged nanocrystal ink may be achieved from a single deposition step, without the need for multiple layer-by-layer deposition cycles often implemented in QD devices. Lateral photoconductive devices formed from the inks showcase high on/off ratios and fast response times, highlighting the applicability in photodetection domain. Given the established role of surface ligands in tuning band edge energy levels in deposited films,[14] we postulate that the inclusion of mild proton donating additives during phase transfer ligand exchange processes could offer benefits in both the processing time and tuning the electronic properties of QD films. This work provides encouraging evidence for further developments in environmentally benign ternary QD inks for state-of-the-art lightweight, low-power solution processed electronics and optoelectronics, where the advantages in scalable deposition processes such as inkjet printing or spray coating may be realized to overcome limitations of SSLE methods or other solution phase fabrication routes requiring multilayer steps.

■ ASSOCIATED CONTENT

Supporting Information

The Supporting Information is available free of charge at https://pubs.acs.org/doi/10.1021/acsaelm.0c01107.

Materials and detailed methods for synthesis, purification, and phase transfer of $AgBiS_2$ QDs; electronic device fabrication and measurement techniques; Figures S1 and S2 (PDF)

■ AUTHOR INFORMATION

Corresponding Author

Andrew B. Greytak − *Department of Chemistry and Biochemistry, University of South Carolina, Columbia, South Carolina 29208, United States;* orcid.org/0000-0001-8978-6457; Email: greytak@sc.edu

Authors

Mathew L. Kelley − *Department of Chemistry and Biochemistry, University of South Carolina, Columbia, South Carolina 29208, United States;* orcid.org/0000-0002-6940-4148

Fiaz Ahmed − *Department of Chemistry and Biochemistry, University of South Carolina, Columbia, South Carolina 29208, United States;* orcid.org/0000-0002-6977-3672

Sakiru L. Abiodun − *Department of Chemistry and Biochemistry, University of South Carolina, Columbia, South Carolina 29208, United States*

Mohammad Usman − *Department of Chemistry and Biochemistry, University of South Carolina, Columbia, South Carolina 29208, United States*

Mohi Uddin Jewel − *Department of Electrical and Computer Engineering, University of South Carolina, Columbia 29208, United States*

Kamal Hussain − *Department of Chemistry and Biochemistry, University of South Carolina, Columbia, South Carolina 29208, United States*

Hans-Conrad zur Loye − *Department of Chemistry and Biochemistry, University of South Carolina, Columbia, South Carolina 29208, United States;* orcid.org/0000-0001-7351-9098

M. V. S. Chandrashekhar − *Department of Electrical and Computer Engineering, University of South Carolina, Columbia 29208, United States*

Complete contact information is available at: https://pubs.acs.org/10.1021/acsaelm.0c01107

Notes

The authors declare no competing financial interest.

■ ACKNOWLEDGMENTS

This work was supported by the NSF through Grant EPMD-1711322 to A.B.G. and M.V.S.C. Additional support from NSF EPSCOR Track 1 program OIA-1655740 is acknowledged by A.B.G. and H.C.z.L. We thank Corey Martin and Logan Breton for helpful discussions.

■ REFERENCES

(1) Talapin, D. V.; Lee, J.-S.; Kovalenko, M. V.; Shevchenko, E. V. Prospects of Colloidal Nanocrystals for Electronic and Optoelectronic Applications. *Chem. Rev.* **2010**, *110* (1), 389−458.

(2) Jiang, L.; Li, Y.; Peng, J.; Cui, L.; Li, R.; Xu, Y.; Li, W.; Li, Y.; Tian, X.; Lin, Q. Solution-Processed $AgBiS_2$ Photodetectors from Molecular Precursors. *J. Mater. Chem. C* **2020**, *8* (7), 2436−2441.

(3) Viñes, F.; Konstantatos, G.; Illas, F. Bandgap Engineering by Cationic Disorder: Case Study on $AgBiS_2$. *Phys. Chem. Chem. Phys.* **2017**, *19* (41), 27940−27944.

(4) Öberg, V. A.; Johansson, M. B.; Zhang, X.; Johansson, E. M. J. Cubic $AgBiS_2$ Colloidal Nanocrystals for Solar Cells. *ACS Appl. Nano Mater.* **2020**, *3* (5), 4014−4024.

(5) Bernechea, M.; Miller, N. C.; Xercavins, G.; So, D.; Stavrinadis, A.; Konstantatos, G. Solution-Processed Solar Cells Based on Environmentally Friendly $AgBiS_2$ Nanocrystals. *Nat. Photonics* **2016**, *10* (8), 521−525.

(6) Chen, C.; Qiu, X.; Ji, S.; Jia, C.; Ye, C. The Synthesis of Monodispersed $AgBiS_2$ Quantum Dots with a Giant Dielectric Constant. *CrystEngComm* **2013**, *15* (38), 7644−7648.

(7) Mak, C. H.; Qian, J.; Rogée, L.; Lai, W. K.; Lau, S. P. Facile Synthesis of $AgBiS_2$ Nanocrystals for High Responsivity Infrared Detectors. *RSC Adv.* **2018**, *8* (68), 39203−39207.

(8) Kagan, C. R.; Murray, C. B. Charge Transport in Strongly Coupled Quantum Dot Solids. *Nat. Nanotechnol.* **2015**, *10* (12), 1013−1026.

(9) Kirmani, A. R. Commercializing Colloidal Quantum Dot Photovoltaics. *MRS Bull.* **2019**, *44* (7), 524−525.

(10) Fafarman, A. T.; Koh, W.; Diroll, B. T.; Kim, D. K.; Ko, D.-K.; Oh, S. J.; Ye, X.; Doan-Nguyen, V.; Crump, M. R.; Reifsnyder, D. C.; Murray, C. B.; Kagan, C. R. Thiocyanate-Capped Nanocrystal Colloids: Vibrational Reporter of Surface Chemistry and Solution-Based Route to Enhanced Coupling in Nanocrystal Solids. *J. Am. Chem. Soc.* **2011**, *133* (39), 15753−15761.

(11) Sayevich, V.; Gaponik, N.; Plötner, M.; Kruszynska, M.; Gemming, T.; Dzhagan, V. M.; Akhavan, S.; Zahn, D. R. T.; Demir, H. V.; Eychmüller, A. Stable Dispersion of Iodide-Capped PbSe Quantum Dots for High-Performance Low-Temperature Processed Electronics and Optoelectronics. *Chem. Mater.* **2015**, *27* (12), 4328−4337.

(12) Nag, A.; Kovalenko, M. V.; Lee, J.-S.; Liu, W.; Spokoyny, B.; Talapin, D. V. Metal-Free Inorganic Ligands for Colloidal Nanocrystals: S^{2-}, HS^-, Se^{2-}, HSe^-, Te^{2-}, HTe^-, TeS_3^{2-}, OH^-, and NH^{2-} as Surface Ligands. *J. Am. Chem. Soc.* **2011**, *133* (27), 10612−10620.

(13) Zhang, H.; Jang, J.; Liu, W.; Talapin, D. V. Colloidal Nanocrystals with Inorganic Halide, Pseudohalide, and Halometallate Ligands. *ACS Nano* **2014**, *8* (7), 7359−7369.

(14) Kroupa, D. M.; Vörös, M.; Brawand, N. P.; McNichols, B. W.; Miller, E. M.; Gu, J.; Nozik, A. J.; Sellinger, A.; Galli, G.; Beard, M. C. Tuning Colloidal Quantum Dot Band Edge Positions through Solution-Phase Surface Chemistry Modification. *Nat. Commun.* **2017**, *8*, 15257.

(15) Lee, S.; Choi, M.-J.; Sharma, G.; Biondi, M.; Chen, B.; Baek, S.-W.; Najarian, A. M.; Vafaie, M.; Wicks, J.; Sagar, L. K.; Hoogland, S.; de Arquer, F. P. G.; Voznyy, O.; Sargent, E. H. Orthogonal Colloidal Quantum Dot Inks Enable Efficient Multilayer Optoelectronic Devices. *Nat. Commun.* **2020**, *11* (1), 4814.

(16) Giansante, C.; Carbone, L.; Giannini, C.; Altamura, D.; Ameer, Z.; Maruccio, G.; Loiudice, A.; Belviso, M. R.; Cozzoli, P. D.; Rizzo, A.; Gigli, G. Colloidal Arenethiolate-Capped PbS Quantum Dots: Optoelectronic Properties, Self-Assembly, and Application in Solution-Cast Photovoltaics. *J. Phys. Chem. C* **2013**, *117* (25), 13305−13317.

(17) Song, J. H.; Choi, H.; Pham, H. T.; Jeong, S. Energy Level Tuned Indium Arsenide Colloidal Quantum Dot Films for Efficient Photovoltaics. *Nat. Commun.* **2018**, *9* (1), 4267.

(18) Choi, M.-J.; García de Arquer, F. P.; Proppe, A. H.; Seifitokaldani, A.; Choi, J.; Kim, J.; Baek, S.-W.; Liu, M.; Sun, B.; Biondi, M.; Scheffel, B.; Walters, G.; Nam, D.-H.; Jo, J. W.; Ouellette, O.; Voznyy, O.; Hoogland, S.; Kelley, S. O.; Jung, Y. S.; Sargent, E. H. Cascade Surface Modification of Colloidal Quantum Dot Inks Enables Efficient Bulk Homojunction Photovoltaics. *Nat. Commun.* **2020**, *11* (1), 103.

(19) Lin, Q.; Yun, H. J.; Liu, W.; Song, H.-J.; Makarov, N. S.; Isaienko, O.; Nakotte, T.; Chen, G.; Luo, H.; Klimov, V. I.; Pietryga, J. M. Phase-Transfer Ligand Exchange of Lead Chalcogenide Quantum Dots for Direct Deposition of Thick, Highly Conductive Films. *J. Am. Chem. Soc.* **2017**, *139* (19), 6644−6653.

(20) Liu, M.; Voznyy, O.; Sabatini, R.; García de Arquer, F. P.; Munir, R.; Balawi, A. H.; Lan, X.; Fan, F.; Walters, G.; Kirmani, A. R.; Hoogland, S.; Laquai, F.; Amassian, A.; Sargent, E. H. Hybrid Organic-Inorganic Inks Flatten the Energy Landscape in Colloidal Quantum Dot Solids. *Nat. Mater.* **2017**, *16* (2), 258−263.

(21) Choi, H.; Kim, S.; Luther, J. M.; Kim, S.-W.; Shin, D.; Beard, M. C.; Jeong, S. Facet-Specific Ligand Interactions on Ternary $AgSbS_2$ Colloidal Quantum Dots. *Chem. - Eur. J.* **2017**, *23* (70), 17707−17713.

(22) Reinhold, H.; Mikolajczak, U.; Brand, I.; Dosche, C.; Borchert, H.; Parisi, J.; Scheunemann, D. Shorter Is Not Always Better: Analysis of a Ligand Exchange Procedure for $CuInS_2$ Nanoparticles as the Photovoltaic Absorber Material. *J. Phys. Chem. C* **2020**, *124* (37), 19922−19928.

(23) Bae, S. Y.; Oh, J. T.; Park, J. Y.; Ha, S. R.; Choi, J.; Choi, H.; Kim, Y. Improved Eco-Friendly Photovoltaics Based on Stabilized $AgBiS_2$ Nanocrystal Inks. *Chem. Mater.* **2020**, *32*, 10007.

(24) Jo, J. W.; Choi, J.; García de Arquer, F. P.; Seifitokaldani, A.; Sun, B.; Kim, Y.; Ahn, H.; Fan, J.; Quintero-Bermudez, R.; Kim, J.; Choi, M.-J.; Baek, S.-W.; Proppe, A. H.; Walters, G.; Nam, D.-H.; Kelley, S.; Hoogland, S.; Voznyy, O.; Sargent, E. H. Acid-Assisted Ligand Exchange Enhances Coupling in Colloidal Quantum Dot Solids. *Nano Lett.* **2018**, *18* (7), 4417−4423.

(25) Ming, S.; Liu, X.; Zhang, W.; Xie, Q.; Wu, Y.; Chen, L.; Wang, H.-Q. Eco-Friendly and Stable Silver Bismuth Disulphide Quantum Dot Solar Cells via Methyl Acetate Purification and Modified Ligand Exchange. *J. Cleaner Prod.* **2020**, *246*, 118966.

(26) van Embden, J.; Della Gaspera, E. Ultrathin Solar Absorber Layers of Silver Bismuth Sulfide from Molecular Precursors. *ACS Appl. Mater. Interfaces* **2019**, *11* (18), 16674−16682.

(27) Geller, S.; Wernick, J. H. Ternary Semiconducting Compounds with Sodium Chloride-like Structure: $AgSbSe_2$, $AgSbTe_2$, $AgBiS_2$, $AgBiSe_2$. *Acta Crystallogr.* **1959**, *12* (1), 46−54.
(28) Jia, D.; Chen, J.; Zheng, S.; Phuyal, D.; Yu, M.; Tian, L.; Liu, J.; Karis, O.; Rensmo, H.; Johansson, E. M. J.; Zhang, X. Highly Stabilized Quantum Dot Ink for Efficient Infrared Light Absorbing Solar Cells. *Adv. Energy Mater.* **2019**, *9*, 1902809.
(29) Klem, E. J. D.; Shukla, H.; Hinds, S.; MacNeil, D. D.; Levina, L.; Sargent, E. H. Impact of Dithiol Treatment and Air Annealing on the Conductivity, Mobility, and Hole Density in PbS Colloidal Quantum Dot Solids. *Appl. Phys. Lett.* **2008**, *92* (21), 212105.
(30) Medina-Gonzalez, A. M.; Rosales, B. A.; Hamdeh, U. H.; Panthani, M. G.; Vela, J. Surface Chemistry of Ternary Nanocrystals: Engineering the Deposition of Conductive $NaBiS_2$ Films. *Chem. Mater.* **2020**, *32*, 6085.
(31) Gu, E.; Lin, X.; Tang, X.; Matt, G. J.; Osvet, A.; Hou, Y.; Jäger, S.; Xie, C.; Karl, A.; Hock, R.; Brabec, C. J. Single Molecular Precursor Ink for $AgBiS_2$ Thin Films: Synthesis and Characterization. *J. Mater. Chem. C* **2018**, *6* (28), 7642−7651.
(32) Kelley, M. L.; Letton, J.; Simin, G.; Ahmed, F.; Love-Baker, C. A.; Greytak, A. B.; Chandrashekhar, M. V. S. Photovoltaic and Photoconductive Action Due to PbS Quantum Dots on Graphene/SiC Schottky Diodes from NIR to UV. *ACS Appl. Electron. Mater.* **2020**, *2* (1), 134−139.
(33) Strasfeld, D. B.; Dorn, A.; Wanger, D. D.; Bawendi, M. G. Imaging Schottky Barriers and Ohmic Contacts in PbS Quantum Dot Devices. *Nano Lett.* **2012**, *12* (2), 569−575.

https://doi.org/10.1021/acsaelm.0c01107
ACS Appl. Electron. Mater. 2021, 3, 1550−1555